Inorg. Chem. **2004**, *43*, 8379–8386

Synthesis, Crystal Structure from Single-Crystal and Powder X-ray Diffraction Data, and Thermal Behavior of Mixed Potassium Lanthanide Squarates: Thermal Transformations of Layered $[Ln(H_2O)_6]K(H_2C_4O_4)(C_4O_4)_2$ into Pillared $LnK(C_4O_4)_2$ (Ln = Y, La, Gd, Er)

Nathalie Mahé and Thierry Bataille*

Laboratoire de Chimie du Solide et Inorganique Moléculaire (UMR 6511 CNRS), Institut de Chimie, Université de Rennes 1, Avenue du Général Leclerc, 35042 Rennes, France

Received August 14, 2004

A new series of mixed potassium and rare-earth squarates, $[Ln(H_2O)_6]K(H_2C_4O_4)(C_4O_4)_2$ (Ln = Y, La, Gd, Er), has been synthesized and structurally characterized from single-crystal X-ray diffraction and spectroscopic analyses. The yttrium-based compound crystallizes with a monoclinic symmetry, space group *C*2/*c* [a = 8.3341(2) Å, b = 37.7094(9) Å, c = 11.7195(3) Å, β = 90.3959(9)°, V = 3683.1(2) Å^3, Z = 8]. The structure is built from layers maintained together via hydrogen bonds. Within a layer, squarate ligands act as linkers between lanthanide and potassium cations. The thermal decomposition of the precursors has been studied by powder thermodiffractometry and thermal analyses. It is shown that crystalline intermediate phases are formed during the degradation. Among them, unprecedented mixed anhydrous squarates, $LnK(C_4O_4)_2$, could be isolated. The crystal structure of the Y compound has been solved ab initio from X-ray powder diffraction data, using direct-space methods [a = 6.2010(5) Å, c = 11.639(1) Å, V = 447.55 Å^3, Z = 2]. The structure consists of layers of edge-sharing YO_8 and KO_8 antiprisms, pillared by μ_8-squarate groups. The end of the precursor decomposition is marked by the formation of cubic sesquioxides Ln_2O_3, including lanthanum oxide.

Introduction

In the recent years, the use of oxocarbon entities, as carboxylates, in inorganic synthesis has spectacularly increased. One of the major interests in the application of such ligands is the diversity of their design to conceive new architectures, e.g., toward very opened frameworks and porous materials.[1] Prior to this effervescence, the literature has been enriched by many oxocarbon-based compounds possessing interesting structural features, such as salts of 3,4-dihydroxy-3-cyclobutene-1,2-dione ($H_2C_4O_4$), also known as squarates. Indeed, there have been reported chains,[2] layers,[3] and three-dimensional[3,4] squarates exhibiting zeolitic,[5] magnetic,[6] or luminescent[7] properties. Our previous studies based on new mixed metal oxalate compounds demonstrated that it could be possible to rationally elaborate nanoporous materials having zeolitic and ion exchange properties.[8] These phases adopt the structure type of $YK(C_2O_4)_2{\cdot}4H_2O$.[9] In this structure, Y and K are connected by bischelating oxalate

* Author to whom correspondence should be addressed. E-mail: thierry.bataille@univ-rennes1.fr.

(1) (a) Chae, H. K.; Siberio-Perez, D. Y.; Kim, J.; Go, Y.; Eddaoudi, M.; Matzger, A. J.; O'Keeffe, M.; Yaghi, O. M. *Nature* **2004**, *427*, 523−527. (b) Rowsell, J. L. C.; Yaghi, O. M. *Microporous Mesoporous Mater.* **2004**, *73*, 3−14 and references therein. (c) Rao, C. N. R.; Natarajan, S.; Vaidhyanathan, R. *Angew. Chem., Int. Ed.* **2004**, *43*, 1466−1496. (d) Loiseau, T.; Serre, C.; Huguenard, C.; Fink, G.; Taulelle, F.; Henry, M.; Bataille, T.; Férey, G. *Chem.—Eur. J.* **2004**, *10*, 1373−1382. (e) Guillou, N.; Livage, C.; Drillon, M.; Férey, G. *Angew. Chem., Int. Ed.* **2003**, *42*, 5314−5317. (f) Neeraj, S.; Noy, M. L.; Rao, C. N. R.; Cheetham, A. K. *Solid State Sci.* **2002**, *4*, 1231−1236.

(2) Van Ooijen, J. A. C.; Reedijk, J.; Spek, A. L. *Inorg. Chem.* **1979**, *18*, 1184−1189.

(3) Lin, K.-J.; Lii, K.-H. *Angew. Chem., Int. Ed. Engl.* **1997**, *36*, 2076−2077.

(4) (a) Gutschke, S. O. H.; Molinier, M.; Powell, A. K.; Wood, P. T. *Angew. Chem., Int. Ed. Engl.* **1997**, *36*, 991−992. (b)Robl C.; Gnutzmann, V.; Weiss, A. *Z. Anorg. Allg. Chem.* **1987**, *549*, 187−194.

(5) Robl, C.; Weiss, A. *Mater. Res. Bull.* **1987**, *22*, 373−380.

(6) Bouayad, A.; Brouca-Cabarrecq, C.; Trombe, J.-C.; Gleizes, A. *Inorg. Chim. Acta* **1992**, *195*, 193−201.

(7) De Mello Donega, C.; Ribeiro, S. J. L.; Goncalves, R. R.; Blasse, G. *J. Phys. Chem. Solids* **1996**, *57*, 1727−1734.

(8) Audebrand, N.; Jeanneau, E.; Bataille, T.; Raite, S.; Louër, D. *Solid State Sci.* **2004**, *6*, 579−591.

(9) Bataille, T.; Auffrédic, J.-P., Louër, D. *Chem. Mater.* **1999**, *11*, 1559−1567.

10.1021/ic0488839 CCC: $27.50
Published on Web 11/23/2004

Table 1. Refined Unit Cell Parameters of the Isostructural Compounds $[Ln(H_2O)_6]K(H_2C_4O_4)(C_4O_4)_2$ from X-ray Powder Diffraction Data

	Ln^{3+}			
	La	Gd	Er	Y
a (Å)	8.3398(2)	8.3368(6)	8.3303(2)	8.3371(2)
b (Å)	37.6962(7)	37.793(2)	37.6453(6)	37.6946(9)
c (Å)	11.7141(2)	11.7272(7)	11.7082(3)	11.7197(2)
β (deg)	90.512(2)	90.337(6)	90.316(2)	90.463(2)
V (Å^3)	3682	3695	3672	3683

groups to form a three-dimensional network displaying tunnels. On the other hand, it has been shown in the past that the squarate ligand could connect metal atoms in a bidentate fashion.[10] In particular, it has been suggested that chelating and bischelating coordination modes are only possible in the presence of large cations, such as alkaline-earth[5] and rare-earth elements.[11] Thus, it was of interest to synthesize new mixed rare-earth materials using the squarate entity, to obtain porous materials similar to the related oxalate phases. Although several lanthanide squarate structures have been reported in the literature,[12] only few of them are built from rare-earth and metal cations.[6] Here, new layered compounds with the chemical formula $[Ln(H_2O)_6]K(H_2C_4O_4)(C_4O_4)_2$ (Ln = Y, La, Gd, Er) have been prepared. This study deals with their synthesis and structure determination, as well as their thermal behavior reported from thermal analyses and thermodiffractometry. In addition, the power of recent methods in powder crystallography is demonstrated by the structure determination of unprecedented mixed anhydrous squarates obtained by thermal degradation of the microcrystalline precursors.

Experimental Section

Materials. All chemicals were commercially available and used as received. For convenience, 3,4-dihydroxy-3-cyclobutene-1,2-dione ($H_2C_4O_4$) is named squaric acid hereafter. The other reagents were $Ln_2(SO_4)_3{\cdot}8H_2O$, with Ln = Er and Gd, $La(NO_3)_3{\cdot}6H_2O$, $Y(NO_3)_3{\cdot}5H_2O$, and KNO_3.

Synthesis of $[Ln(H_2O)_6]K(H_2C_4O_4)(C_4O_4)_2$, with Ln = Y, La, Gd, and Er. The compounds were obtained as precipitates. The rare-earth salt (1 mmol of Ln^{3+}) and KNO_3 (2 mmol) were dissolved in 20 mL of distilled water. A 20 mL volume of an aqueous solution containing 2 mmol of squaric acid was added dropwise to the former one. The batch was vigorously stirred until a precipitate appeared after a few moments. The powder was recovered by filtration and dried in air. The X-ray powder diffraction patterns indicated that the compounds are isostructural. The chemical formula was derived from the Ln:K ratio (1:1) obtained by energy dispersive X-ray spectrometry, performed with a JSM 6400 spectrometer equipped with an Oxford Link Isis analyzer, and from the crystal structure determination reported below. It is in agreement with the chemical formula $[Ln(H_2O)_6]K(H_2C_4O_4)(C_4O_4)_2$. Table 1 displays the unit cell parameters of the isostructural compounds, derived from least-squares refinements from X-ray powder diffraction data. Single crystals of the yttrium compound could be also obtained as follows: a mixture of $H_2C_4O_4$ (2 mmol) and KNO_3 (2 mmol) was dissolved in 20 mL of distilled water. A 5 mL aqueous solution of $Y(NO_3)_3{\cdot}5H_2O$ (1 mmol) was then added dropwise. The cleared solution was allowed to stand at room temperature. After 1 day, long and thin colorless needles appeared. The crystals were filtered off, thoroughly washed with distilled water, and dried in air. The X-ray powder diffraction pattern of the milled crystals indicated that the product was identical with the powdered phases. It was subsequently verified that the powder patterns were in agreement with the pattern calculated from the single-crystal structure determination.

Preparation of $LnK(C_4O_4)_2$, with Ln = Y, La, Gd, and Er. These compounds were obtained from the decomposition of the precursors, $[Ln(H_2O)_6]K(H_2C_4O_4)(C_4O_4)_2$. For the yttrium-based compound, the white powdered precursor was heated in a tubular oven under flowing air, at 10 °C h^{-1} up to 240 °C, and kept during 36 h at this temperature. The decomposition product is a brown disperse powder stable at room temperature. The X-ray diffraction pattern indicated that it is a new material. The chemical formula was derived from energy dispersive X-ray spectrometry (ratio Y:K = 1:1), temperature-dependent X-ray diffraction, and the result of thermogravimetric measurements. It is in agreement with the chemical composition $YK(C_4O_4)_2$.

Single-Crystal Data Collection and Structure Determination of $[Y(H_2O)_6]K(H_2C_4O_4)(C_4O_4)_2$. A suitable crystal was glued to a glass fiber mounted on a four-circle Nonius Kappa CCD area-detector diffractometer. Intensity data sets were collected using Mo Kα radiation (λ = 0.710 73 Å) through the program COLLECT.[13] Correction for the Lorentz−polarization effect, peak integration, and background determination were carried out with the program DENZO.[14] Unit cell parameters refinement were performed with the program SCALEPACK.[14] Numerical absorption correction was performed by modeling the crystal faces.[15] The crystal structure was solved in the monoclinic symmetry, space group $C2/c$ (No. 15). Yttrium and potassium atoms were located using the direct methods with the program SIR97.[16] C and O atoms from the squarate groups, and water molecules including H atoms were found from successive Fourier calculations using SHELXL-97.[17] The two hydrogen atoms situated on the squaric acid molecule were found among the residual electron density peaks displayed around the O atoms. Their positions were validated from geometrical considerations as well as from the examination of possible hydrogen bonds. Within a water molecule, the O−H distance was restrained to 0.97(2) Å and the H−H distance to 1.55(3) Å, so that the H−O−H angle fitted the ideal value of a tetrahedral angle. Within the squaric acid group, the two O−H distances were restrained to 0.97(3) Å. The atomic displacement parameters of the H atoms were fixed at $1.5U_{eq}$ of their parent atom. Crystallographic data are given in Table 2. Selected bond distances and angles, as well as hydrogen bonds, are listed in Tables 3 and 4.

(10) Solans, X.; Aguilo, M.; Gleizes, A.; Faus, J.; Julve, M.; Verdaguer, M. *Inorg. Chem.* **1990**, *29*, 775−784 and references therein.

(11) Trombe, J.-C.; Petit, J.-F.; Gleizes, A. *New J. Chem.* **1988**, *12*, 197−200.

(12) (a) Petit, J.-F.; Gleizes, A.; Trombe, J.-C. *Inorg. Chim. Acta* **1990**, *167*, 51−68. (b) Trombe, J.-C.; Petit, J.-F.; Gleizes, A. *Inorg. Chim. Acta* **1990**, *167*, 69−81. (c) Trombe, J.-C.; Petit, J.-F.; Gleizes, A. *Eur. J. Solid State Inorg. Chem.* **1991**, *28*, 669−681.(d) Heinl, U.; Hinse, P.; Mattes, R. *Z. Anorg. Allg. Chem.* **2001**, *627*, 2173-2177.

(13) *Nonius, Kappa CCD Program Software*; Nonius BV: Delft, The Netherlands, 1998.

(14) Otwinowski, Z.; Minor, W. In *Methods in Enzymology, Vol. 276*; Carter, C. W., Sweet, R. M., Eds.; Academic Press: New York, 1997; pp 307−326.

(15) de Meulenaer, J.; Tompa, H. *Acta Crystallogr.* **1965**, *19*, 1014−1018.

(16) Altomare, A.; Burla, M. C.; Camalli, M.; Cascarano, G. L.; Giacovazzo, C.; Guagliardi, A.; Moliterni, A. G. G.; Polidori, G.; Spagna, R. *J. Appl. Crystallogr.* **1999**, *32*, 115−119.

(17) Sheldrick, G. M.; *SHELXL-97: Program for Crystal Structure Refinement*; University of Göttingen: Göttingen, Germany, 1997.

Table 2. Crystallographic Data for $[Y(H_2O)_6]K(H_2C_4O_4)(C_4O_4)_2$

empirical formula	$C_{12}H_{14}KO_{18}Y$
fw	574.24
cryst system	monoclinic
space group	*C*2/*c* (No. 15)
cryst size, mm	0.3 × 0.05 × 0.03
a, Å	8.3341(2)
b, Å	37.7094(9)
c, Å	11.7195(3)
β, deg	90.3959(9)
V, Å^3	3683.1(2)
Z	8
T, K	293(2)
D_{calc}, g/cm^3	2.071
λ(Mo Kα), Å	0.710 73
μ, mm^{-1}	3.493
θ range, deg	0.994−30.01
index ranges	$-11 \le h \le 9$, $-41 \le k \le 52$, $-16 \le l \le 14$
unique data	5365
obsd data ($I > 2\sigma(I)$)	4026
R_1 ($I > 2\sigma(I)$)	0.0998
R_1 (all)	0.0758
wR_2 ($I > 2\sigma(I)$)	0.1907
wR_2 (all)	0.1796
refinement method	full-matrix least squares on $\|F^2\|$
goodness of fit	1.142
no. of variables	334
no. of restraints	20
largest diff map peak and hole, e Å^{-3}	1.779 and −1.464

Table 3. Selected Bond Lengths (Å) for $[Y(H_2O)_6]K(H_2C_4O_4)(C_4O_4)_2$ [a]

	MO_8 Polyhedra		
Y1−O1W, O1W^{i}	2.419(4)	K1−O5^{i}, O5	2.809(4)
Y1−O1, O1^{i}	2.308(4)	K1−O1W, O1W^{i}	2.974(5)
Y1−O2W^{i}, O2W	2.346(4)	K1−O11, O11^{i}	2.796(4)
Y1−O3W, O3W^{i}	2.362(4)	K1−O9, O9^{i}	2.698(5)
Y2−O4^{ii}, O4^{iv}	2.337(4)	K2−O4W, O4W^{iii}	3.044(5)
Y2−O4W, O4W^{iii}	2.418(4)	K2−O12, O12^{iii}	2.842(4)
Y2−O5W, O5W^{iii}	2.315(4)	K2−O6, O6^{iii}	2.684(5)
Y2−O6W, O6W^{iii}	2.376(4)	K2−O8, O8^{iii}	2.813(5)
	Squarate Groups		
	SQ1		
C1−C2	1.482(8)	C2−C3	1.537(9)
C3−C4	1.470(8)	C4−C1	1.45(1)
C1−O1	1.284(8)	C2−O2	1.200(8)
C3−O3	1.226(7)	C4−O4	1.260(8)
	SQ2		
C5−C6	1.457(7)	C6−C7	1.492(7)
C7−C8	1.462(7)	C8−C5	1.422(8)
C5−O5	1.277(7)	C6−O6^{v}	1.232(7)
C7−O7	1.231(7)	C8−O8	1.286(7)
O5−H5	0.983(1)	O8−H8	0.975(1)
	SQ3		
C9−C10	1.494(8)	C10−C11	1.465(7)
C11−C12	1.435(7)	C12−C9	1.457(8)
C9−O9	1.237(7)	C10−O10	1.230(7)
C11−O11^{vi}	1.282(7)	C12−O12	1.269(7)

[a] Symmetry codes: (i) $1-x, y, {}^1/_2-z$; (ii) $0.5-x, 0.5+y, 0.5-z$; (iii) $-x, y, 0.5-z$; (iv) $-0.5+x, 0.5+y, z$; (v) $1+x, y, z$; (vi) $-1+x, y, z$.

Collection of High-Resolution X-ray Powder Data for $YK(C_4O_4)_2$. High-quality powder data were obtained with a Siemens D500 diffractometer using monochromatic Cu $K\alpha_1$ radiation ($\lambda = 1.5406$ Å) selected with an incident beam curved-crystal germanium monochromator, with the parafocusing Bragg−Brentano geometry whose characteristics have been reported elsewhere.[18] To minimize preferred orientation effects, the powder was mounted in a side-loaded sample holder.[19] The pattern was scanned at room temperature, over the angular range 10−150° (2*θ*), with a step length of 0.03° (2*θ*) and a counting time of 60 s step^{-1}. The stability of the X-ray source was checked by recording again the diffraction lines at low angles. For pattern indexing, the extraction of peak positions was carried out with the Socabim fitting program available in the PC software package Diffrac^{plus} supplied by Bruker AXS. Powder pattern indexing was performed with the program DICVOL04,[20] which is a release of the program DICVOL91,[21] including tolerance of spurious lines, refinement of zero-shift of the pattern, and complete review on the position of the available diffraction lines. Structure determination was carried out using the direct methods program EXPO,[22] including a whole-pattern decomposition iterative algorithm,[23] and with the parallel tempering algorithm available in the global optimization program FOX.[24] Calculations were performed on a personal computer with a AMD Athlon XP 3000+ processor. Structure refinement was achieved with the program FULLPROF[25] available in the software package WINPLOTR.[26] The Rietveld refinement was carried out with a pseudo-Voigt function to describe the individual line profiles. They included a possible variation of the line shape factor according to a linear dependence with 2*θ* angles, as generally observed for Bragg−Brentano data,[18] and the usual quadratic function in tan *θ* to describe the angular dependence of peak widths.[27] The background was modeled with a linear interpolation between refined intensity points. One preferred orientation parameter was adjusted in the direction of the *c* axis. Soft restraints were applied on distances within the squarate group, i.e., 1.50(1) Å for C−C and 1.25(1) Å for C−O. The usual agreement (*R*) indices have been

Table 4. Possible Hydrogen Bonds in $[Y(H_2O)_6]K(H_2C_4O_4)(C_4O_4)_2$ [a]

D-H···A	*d*(D−H) (Å)	*d*(H···A) (Å)	*d*(D···A) (Å)	∠(D-H···A) (deg)
O1W−H11···O10^{i}	0.97(2)	1.86(4)	2.776(6)	157(7)
O1W−H12···O7^{ii}	0.97(2)	2.00(2)	2.962(7)	174(6)
O2W−H21···O2	0.96(2)	1.78(3)	2.720(7)	165(7)
O2W−H22···O9	0.95(2)	1.80(3)	2.718(6)	162(8)
O3W−H31···O3^{iii}	0.96(2)	1.95(2)	2.909(7)	172(7)
O3W−H32···O2^{i}	0.95(2)	1.77(4)	2.680(7)	159(8)
O4W−H41···O7^{i}	0.97(2)	1.79(2)	2.746(6)	172(7)
O4W−H42···O10^{iv}	0.96(2)	2.09(4)	3.008(7)	158(7)
O5W−H51···O1^{v}	0.98(2)	1.75(3)	2.708(6)	163(6)
O5W−H52···O3^{vi}	1.01(2)	1.75(4)	2.657(6)	147(6)
O6W−H61···O3^{vi}	0.97(2)	2.22(5)	2.990(6)	135(6)
O6W−H62···O6	0.97(2)	1.76(2)	2.730(6)	177(7)
O5−H5···O12^{vii}	0.98(3)	1.52(4)	2.468(6)	161(7)
O8−H8···O11^{vii}	0.98(3)	1.51(3)	2.471(6)	168(8)

[a] Symmetry codes:(i) $-x, y, {}^1/_2-z$; (ii) $1-x, 1-y, 1-z$; (iii) ${}^1/_2+x, {}^1/_2-y, {}^1/_2+z$; (iv) $-x, 1-y, -z$; (v) $1/2-x, {}^1/_2+y, {}^1/_2-z$; (vi) $-{}^1/_2-x, {}^1/_2+y, {}^1/_2-z$; (vii) $1-x, y, {}^1/_2-z$; (viii) $1+x, y, z$.

(18) Louër, D.; Langford, J. I. *J. Appl. Crystallogr.* **1988**, *21*, 430−437.

(19) Swanson, H. E.; Morris, M. C.; Evans, E. H.; Ulmer, L. *Natl. Bur. Stand. (U.S.)* **1964**, *Monogr. 25*, section 3, 1−3.

(20) Boultif, A.; Louër, D. *J. Appl. Crystallogr.* **2004**, *37*, 724−731.

(21) Boultif, A.; Louër, D. *J. Appl. Crystallogr.* **1991**, *24*, 987−993.

(22) Altomare, A.; Burla, M. C.; Camalli, M.; Carrozzini, B.; Cascarano, G. L.; Giacovazzo, C.; Guagliardi, A.; Moliterni, A. G. G.; Polidori, G.; Rizzi, R. *J. Appl. Crystallogr.* **1999**, *32*, 339−340.

(23) Le Bail, A.; Duroy, H.; Fourquet, J. L. *Mater. Res. Bull.* **1988**, *23*, 447−452.

(24) Favre-Nicolin, V.; Cerny, R. *J. Appl. Crystallogr.* **2002**, *35*, 734−743.

(25) Rodriguez-Carvajal, J. In *Abstracts of the Powder Diffraction Meeting*; Galy, J., Louër, D., Eds.; Toulouse, France, 1990; pp 127−128.

(26) Roisnel, T.; Rodriguez-Carvajal, J. *Mater. Sci. Forum* **2001**, *378*−*381*, 118−123.

(27) Caglioti, G.; Paoletti, A.; Ricci, F. P. *Nucl. Instrum.* **1958**, *3*, 223−228.

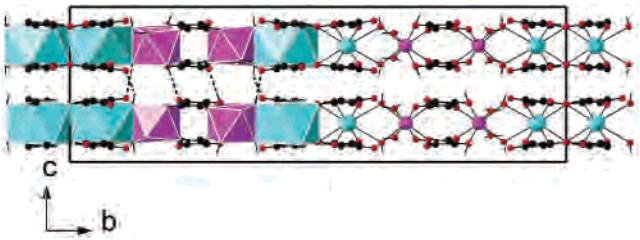

Figure 1. Projection of the structure of $[Y(H_2O)_6]K(H_2C_4O_4)(C_4O_4)_2$ along the *a* axis, showing the layers. Hydrogen bonds are represented by the dotted lines. Key: Y, YO_8, purple; K, KO_8, blue; C, black; O, red; H, white circles.

used (see, for example, ref 28) to quantify the fit of the calculated pattern to the observed data. The program DIAMOND (version 2.1e), supplied by Crystal Impact, was used for structure drawings.

Thermal Analyses. Temperature-dependent X-ray powder diffraction (TDXD) was carried out with a powder diffractometer equipped with a curved position-sensitive detector (INEL CPS120) and a high-temperature attachment from Rigaku. The detector was used in a semifocusing arrangement by reflection (Cu $K\alpha_1$ radiation), as described elsewhere.[29] With this geometry, the stationary sample is deposited on a flat sample holder located at the center of the goniometer. An angle of 6° was selected between the incident beam and the surface of the sample. To ensure satisfactory counting statistics, counting times of 3600 s/pattern were selected for the thermal decomposition of the Y and La precursors. Decompositions were carried out with a heating rate of 3 °C h^{-1} between 18 and 400 °C for $[Y(H_2O)_6]K(H_2C_4O_4)(C_4O_4)_2$ and 3 and 15 °C h^{-1} in the ranges 18−300/300−600 °C for the La-based precursor. Temperature calibration was carried out with standard materials in the involved temperature range.

TG−DTA measurements were performed with a Rigaku Thermoflex instrument in dynamic air. For TG analyses only, the powdered samples were spread evenly in a large crucible to prevent mass effects. For the Y compound, the TG measurement was carried out with heating rates of 3 °C h^{-1} between 18 and 400 °C and 20 °C h^{-1} up to 1000 °C. DTA was performed between 18 and 450 °C at a regime of 2 °C min^{-1}.

Results and Discussion

Structure Description of the Precursor $[Y(H_2O)_6]K(H_2C_4O_4)(C_4O_4)_2$. The two-dimensional crystal structure consists of layers made of yttrium and potassium cations connected by squarate groups (denoted SQ1, SQ2, and SQ3 hereafter) and water molecules and stacked along the *c* axis (Figure 1). Figure 2 shows part of the structure of $[Y(H_2O)_6]K(H_2C_4O_4)(C_4O_4)_2$ projected on the (*ab*) plane. The yttrium cation is coordinated to two squarate oxygen atoms from two squarate units (SQ1) and six water oxygen atoms, while K is surrounded by six squarate oxygen atoms from six squarate groups (SQ2 and SQ3) and two water O atoms only. The 8-fold coordination polyhedra of Y and K can be described as slightly distorted square antiprisms. The Y−O and K−O bond lengths fall into the ranges 2.308(4)−2.419(4) Å ($\langle Y-O\rangle$ = 2.360(4) Å) and 2.684(5)−3.044(5) Å ($\langle K-O\rangle$ = 2.833(5) Å), respectively. These distances are in agreement with the values calculated from the bond

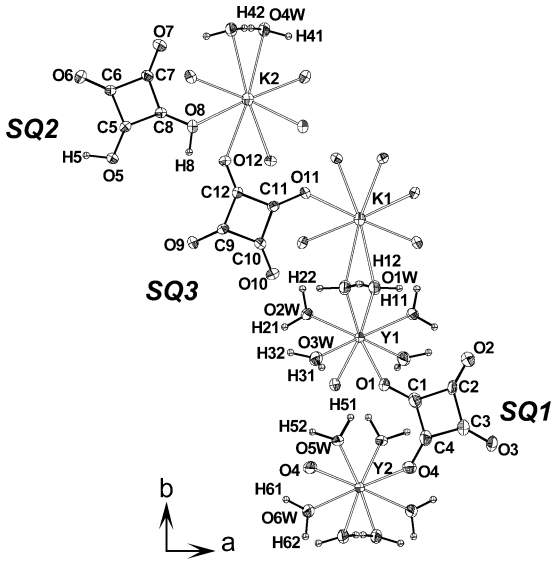

Figure 2. Molecular structure and atom numbering scheme of $[Y(H_2O)_6]K(H_2C_4O_4)(C_4O_4)_2$. Ellipsoids are drawn at the 50% probability level.

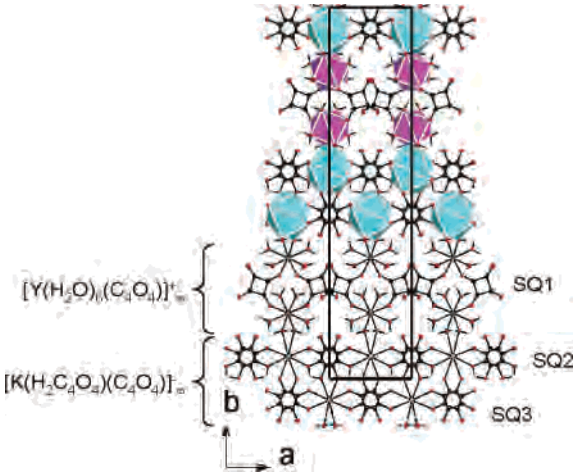

Figure 3. Projection of the structure of $[Y(H_2O)_6]K(H_2C_4O_4)(C_4O_4)_2$ along the *c* axis, showing the ribbons $[Y(H_2O)_6(C_4O_4)]^+_\infty$ and $[K(H_2C_4O_4)(C_4O_4)]^-_\infty$ running along [100].

valence program VALENCE[30] for 8-fold-coordinated Y and K, i.e., 2.382 and 2.901 Å. The squarate units are planar with their mean plane nearly perpendicular to the *c* axis. The three independent squarate groups play different roles in the structure connectivity. The squarate dianion SQ1 is engaged in a μ_2-1,2-bis(monodentate) binding mode. It bridges Y1 and Y2 to form a $[Y_2(H_2O)_{12}(SQ1)_2]$ dimer, thus leading to a ribbon of formula $[Y(H_2O)_6(C_4O_4)]^+_\infty$ running along [100], as seen in Figure 3. The squarate groups SQ2 and SQ3 act as trimonodentate ligands in a μ_3 bridging mode. However, SQ3 is dianionic while SQ2 is diprotonated and corresponds to a squaric acid molecule. The two independent groups are bridging ligands toward three potassium ions. The resulting ribbon, running along [100], consists of a double chain of alternating potassium and squarate entities with the formula $[K(H_2C_4O_4)(C_4O_4)]^-_\infty$ (Figure 3). The two ribbons $[Y(H_2O)_6(C_4O_4)]^+_\infty$ and $[K(H_2C_4O_4)(C_4O_4)]^-_\infty$ are linked together by sharing two water molecules in the direction of the *b* axis to

(28) McCusker, L. B.; Von Dreele, R. B.; Cox, D. E.; Louër, D.; Scardi, P. *J. Appl. Crystallogr.* **1999**, *32*, 36−50.
(29) Auffrédic, J. P.; Plévert, J.; Louër, D. *J. Solid State Chem.* **1990**, *84*, 58−70.
(30) Brown, I. D. *J. Appl. Crystallogr.* **1996**, *29*, 479−480.

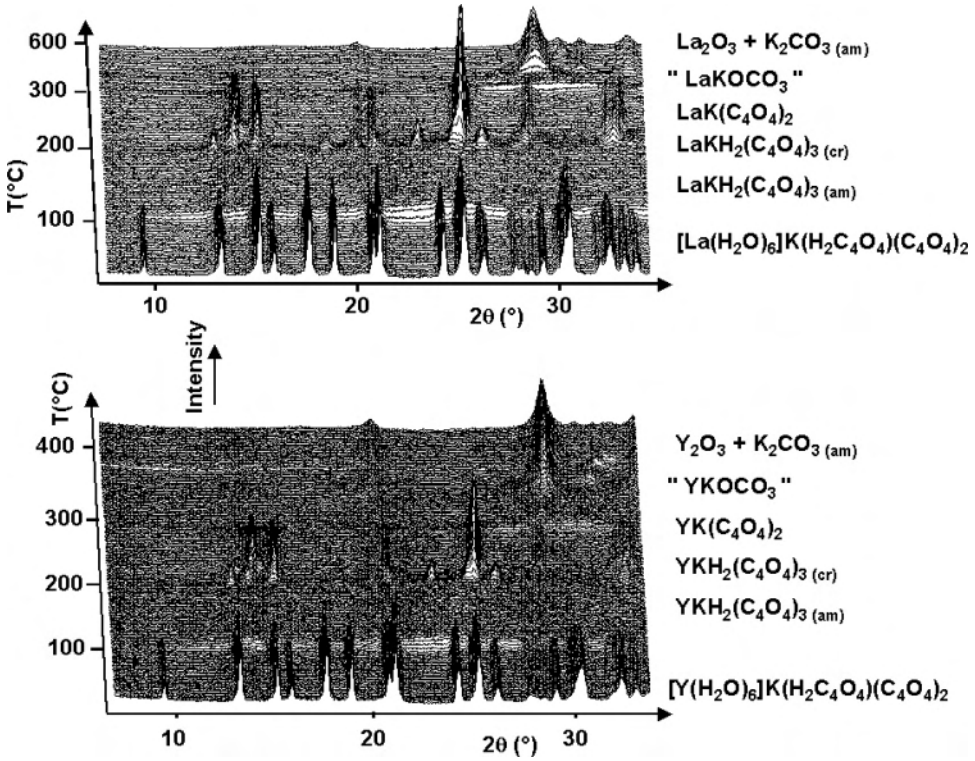

Figure 4. TDXD plots for thermal decomposition of $[La(H_2O)_6]K(H_2C_4O_4)(C_4O_4)_2$ (top) and $[Y(H_2O)_6]K(H_2C_4O_4)(C_4O_4)_2$ (bottom) in air.

build up the layer. As shown in Figures 1 and 3, two neighboring squarate ligands, i.e., SQ2−SQ2 and SQ3−SQ3, stack up within a sheet. They are separated by ca. 3.3 Å and are tilted by an angle of ∼45°. It may be indicative of van der Waals interactions between the two π-systems, as reported previously.[12a] On the contrary, ligand SQ1 is not overlapped. In addition, the squaric acid group SQ2 is hydrogen donor to the ligand SQ3 within a layer (Table 4). The interlayer space is about 2.7 Å, in agreement with the hydrogen bond network involving water molecules between two adjacent layers. Such configuration ensures the stability of the structure, as also observed in cerium or metal squarates.[12b,31]

Thermal Behavior of $[Ln(H_2O)_6]K(H_2C_4O_4)(C_4O_4)_2$ (Ln = Y, La, Gd, Er). The thermal decomposition of $[Ln(H_2O)_6]K(H_2C_4O_4)(C_4O_4)_2$ (Ln = Y, La, Gd, Er) was studied by temperature-dependent X-ray diffraction (TDXD), thermogravimetry (TG), and differential thermal analysis (DTA) under flowing air. Figure 4 shows the successive powder patterns obtained during the thermal decomposition of $[Ln(H_2O)_6]K(H_2C_4O_4)(C_4O_4)_2$ (Ln = Y, La) upon heating. The TG and DTA curves for the Y-based compound are displayed in Figure 5. All the isostructural precursors exhibit similar thermal behaviors. It is shown that the first transformation occurs in the temperature range 90−125 °C, as also revealed by the first endothermic phenomena in the DTA curve. The weight loss of 19.2% is in agreement with the departure of the six water molecules (calculated weight loss, 18.8%), thus leading to the anhydrous phase $YK(H_2C_4O_4)(C_4O_4)_2$, amorphous to X-rays (Figure 4). At 200 °C, some

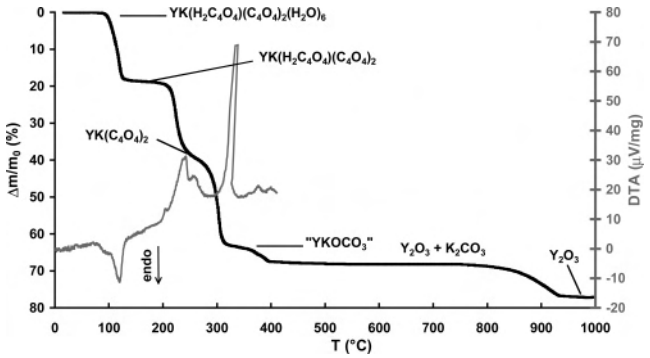

Figure 5. TG and DTA curves for the decomposition of $[Y(H_2O)_6]K(H_2C_4O_4)(C_4O_4)_2$ in air.

diffraction lines emerge from the background. At this temperature no weight loss is observed in the TG curve, while a small exothermic peak is displayed. From these results, it was concluded that the anhydrous phase crystallizes. Unfortunately, the low quality of powder data did not allow further structural investigations on the compound. It can be noted that a similar crystallization behavior has already been observed for the anhydrous lanthanum potassium oxalate.[32] The decomposition of $YK(H_2C_4O_4)(C_4O_4)_2$ starts at 210 °C on the TG curve and leads to a crystalline compound clearly observed between 210 and 300 °C on the TDXD plot. Interrogation of the ICDD Powder Diffraction File[33] revealed that this phase is a new one. To reach its chemical formula, the thermal transformation of the anhydrous phase $YK(H_2C_4O_4)(C_4O_4)_2$ into the present unknown

(31) Lai, S.-F.; Cheng, C.-Y.; Lin, K.-J. *Chem. Commun.* **2001**, 1082−1083.

(32) Bataille, T.; Louër, M.; Auffrédic, J.-P.; Louër, D. *J. Solid State Chem.* **2000**, *150*, 81−95.

(33) International Centre for Diffraction Data, Powder Diffraction File, Newtown Square, PA, 2002.

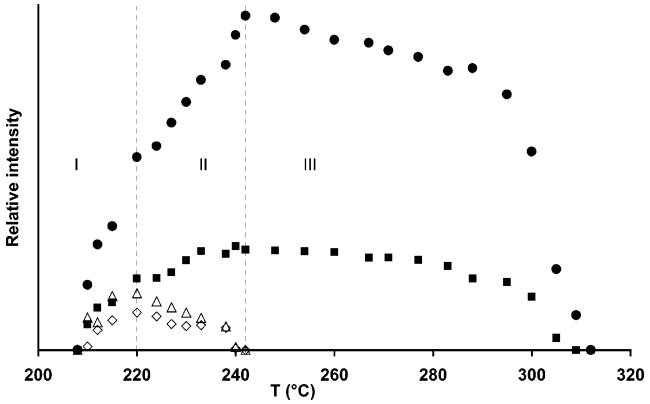

Figure 6. Integrated intensities of selected diffraction lines versus temperature: for $YK(H_2C_4O_4)(C_4O_4)_2$, (◇) line at 13.1° (2θ), (△) line at 23.2° (2θ); for $YK(C_4O_4)_2$, (■) reflection (100), (●) reflection (112). Parts I−III are explained in the text.

compound was investigated from X-ray powder data obtained with the PSD (INEL CPS120). Figure 6 exhibits the changes in integrated intensities of a few diffraction lines selected for the two crystallized phases, as a function of the temperature. It is shown that the Bragg peaks of $YK(H_2C_4O_4)(C_4O_4)_2$ and the new compound appear simultaneously at 210 °C and integrated intensities increase up 220 °C for the two phases (part I). Then, selected integrated intensities for $YK(H_2C_4O_4)(C_4O_4)_2$ vanish up to 240 °C, while those of the new compound continue to increase until this temperature (part II). Peak intensities for the last phase remain almost constant between 240 and 290 °C (part III). This result clearly shows that $YK(H_2C_4O_4)(C_4O_4)_2$ is nutritive to the new material. The final seeding temperature of the unknown compound, i.e., 240 °C, corresponds to the inflection observed in the TG curve. The weight loss of 38.6% is in agreement with the decomposition of one squaric acid molecule (calculated weight loss, 38.7%). Then, it is deduced that the new compound has the global formula $YK(C_4O_4)_2$. It must be noted here that, to our knowledge, it is the first time that an anhydrous mixed rare-earth squarate has been obtained in a crystalline state and structurally characterized. As described below, the diffraction pattern of $YK(C_4O_4)_2$ has been indexed and its crystal structure has been solved ab initio from X-ray powder diffraction data.

The final stages of the decomposition correspond to the degradation of the remaining squarate groups between 250 and 320 °C to give a product with the global composition "$YKOCO_3$" (observed weight loss 64.4%, calculated weight loss 64.5%). It decomposes in the temperature range 340−400 °C into cubic Y_2O_3, as shown by the appearance of diffraction lines on the TDXD plot. The presence of K_2CO_3, amorphous to X-rays, is expected to balance the observed weight loss (69.8%). Finally, the TG curve shows the decomposition of K_2CO_3 between 750 and 940 °C (observed/calculated weight losses, 78.8/80.3%). It is noteworthy here that cubic sesquioxides Ln_2O_3 are also formed during the decomposition of analogous phases of La, Er, and Gd. Though it is not surprising for the two last elements, the formation of cubic La_2O_3, whose structure is that of the Y-based compound, is outstanding. Indeed, this metastable polymorph variety of lanthanum oxide has only been reported a few times in the literature.[34]

Ab Initio Structure Determination of $YK(C_4O_4)_2$ from X-ray Powder Diffraction Data. The first 20 lines of the powder pattern were indexed on the basis of a tetragonal solution, and the complete review and least-squares refinement of the 32 diffraction lines available led to the unit cell dimensions $a = 6.2010(5)$ Å, $c = 11.639(1)$ Å, and $V = 447.55$ Å^3 [$M_{20} = 64$, $F_{32} = 36(0.010,85)$, refined zero-shift 0.0075° (2θ)]. As for a majority of decomposition products, the powder pattern of $YK(C_4O_4)_2$ exhibits a significant diffraction line broadening, which was estimated to be five times larger than that of the standard reference material LaB_6 (NIST SRM 660a). Consequently, the small number of Bragg positions arising from the small volume and the high symmetry of the compound, combined with broadened lines, did not allow the determination of the space group. The only unambiguous condition for extinction of reflections 0*kl* with $l = 2n + 1$ led to 11 possible space groups. Structure determination was first attempted with the direct methods program EXPO. For each selected space group, integrated intensities were extracted from the pattern−decomposition iterative algorithm implemented in EXPO. The structure factor amplitudes so obtained were used to determine the structure with the direct methods. The heavy Y and K atoms were easily located at their actual special positions (see Table 6, below), while some high electron density peaks could be attributed to carbon and oxygen atoms of the squarate anions, with regard to Y−O and C−O interatomic distances. Whatever selected space group, the model revealed that the squarate group was not planar and the C−C bond lengths were much shorter than expected. Attempts to solve the structure with the orthorhombic symmetry were also unsuccessful. Consequently, structure solution from the recent direct-space methods, i.e., the parallel tempering algorithm available in FOX, was considered. Indeed, recently, this approach has been successfully evaluated for structure determination of decomposition products in case of severe diffraction line broadening.[35] The line profile parameters, zero point, unit cell parameters, and background intensities were preliminary estimated by means of the "pattern matching" option available in FULLPROF. To overcome false solutions arising from the uncertainty of the space group symmetry, a global optimization was performed on the basis of triclinic space group *P*1. The starting configuration was made of two Y and two K atoms and four squarate groups randomly positioned within the pseudotriclinic unit cell. A suitable solution was found after 6.3 million trials, corresponding to 10 hours of calculation, with $R_{wp} = 0.17$. From the positions of similar atoms exhibiting possible relationships, the transformation matrix [1, 0, 0/0, −1, 0/0, 0, −1] was deduced. It was applied to the overall atomic positions displayed by the program FOX. Such symmetry-equivalent positions allowed to find out the correct tetragonal space

(34) Gobichon, A. E.; Auffrédic, J.-P.; Louër, D. *J. Solid State Chem.* **1999**, *144*, 68−80.
(35) Bataille, T.; Audebrand, N.; Boultif, A.; Louër, D. *Z. Kristallogr.* **2004**, in press.

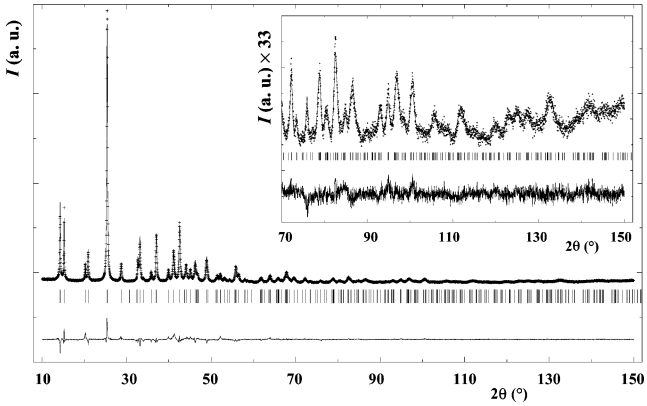

Figure 7. Final Rietveld plot for $YK(C_4O_4)_2$. The experimental data are represented by crosses, while the calculated pattern is shown by the solid line. The lower trace corresponds to the difference curve between observed and calculated patterns. The Bragg reflections are shown by the vertical bars.

Table 5. Crystallographic Data and Details of the Rietveld Refinement for $YK(C_4O_4)_2$

empirical formula	C_8KO_8Y
fw	352.09
cryst system	tetragonal
space group	*P*4/*mcc* (No. 124)
a, Å	6.2010(5)
c, Å	11.639(1)
V, Å^3	447.55
Z	2
wavelength, Å	1.5406
2θ range, deg	10−50
no. of atoms	4
no. of reflcns	269
no. of struct params	11
no. of profile params	22
R_F	0.035
R_B	0.071
R_p	0.077
R_{wp}	0.098
R_{exp}	0.053

group *P*4/*mcc*. It was then necessary to apply the origin-shifted matrix [−0.0680, −0.0202, −0.0576] to the atomic positions in order to obey special Wyckoff positions and symmetry operators in the new space group symmetry. The new positions were used for Rietveld refinement in the actual space group *P*4/*mcc*, which converged to satisfactory *R* values. Figure 7 shows the best agreement obtained between observed and calculated patterns. Crystallographic data and results of the refinement are given in Table 5. Final atomic coordinates and bond distances and angles are displayed in Table 6.

Structure Description of $YK(C_4O_4)_2$. The three-dimensional crystal structure possesses a strong 2D character. It is built from layers of edge-sharing YO_8 and KO_8 polyhedra, pillared by the squarate groups along the *c* axis (Figure 8). Within a layer, the yttrium and potassium cations alternate along the directions [110] and [$\bar{1}$10] (Figure 9). Due to their special positions in space group *P*4/*mcc*, they play an identical role in the formation of the sheet. Thus, they adopt a similar environment, i.e., a square antiprism formed by eight oxygen atoms arising from eight monodentate squarate anions. The four oxygen atoms of the squarate anion are all both connected to one Y and one K atom, so that the squarate molecule adopts an unexpected μ_8 coordination mode. To

Table 6. (a) Atomic Coordinates and Isotropic Atomic Displacement Parameters and (b) Selected Bond Lengths (Å) for $YK(C_4O_4)_2$

(a) Coordinates and Displacement Parameters

atom	*x*/*a*	*y*/*b*	*z*/*c*	B_{iso} (Å^2)
Y	$^1/_2$	$^1/_2$	$^3/_4$	1.08(5)
K	0	0	$^1/_4$	1.24(9)
C	0.4284(8)	0.0876(8)	0.4386(3)	1.2(1)
O	0.3327(5)	0.2105(5)	0.3614(2)	2.1(1)

(b) Bond Lengths[a]

Y−O	2.446(3)	K−O	2.765(3)
C−C^i	1.404(7)	C−O	1.319(5)
C−C^{ii}	1.430(5)		

[a] Symmetry codes: (i) $1 - x, -y, z$; (ii) $x, y, 1 - z$.

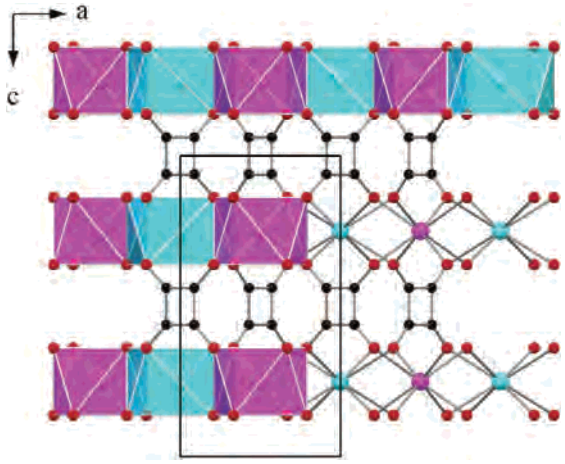

Figure 8. Projection of the structure of $YK(C_4O_4)_2$ along the *b* axis, showing the μ_8 connection of the squarate pillar: Y, YO_8, purple; K, KO_8, blue; C, black; O, red circles.

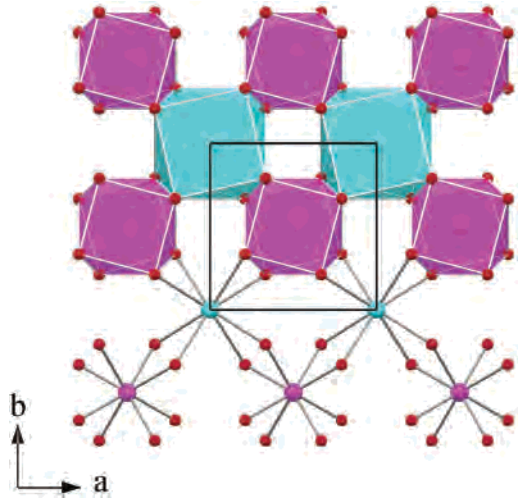

Figure 9. Projection of the structure of $YK(C_4O_4)_2$ along the *c* axis, showing the connectivity between the YO_8 and KO_8 antiprisms within a layer.

the best of our knowledge, this feature is remarkable since it is currently stated that the squarate dianion acts as a μ_1 to μ_6 bridging ligand.[36] Indeed, it has only been encountered with a μ_8 coordination type for $Ba(C_4O_4)$[37] and $Ag_2(C_4O_4)$.[38] Furthermore, the pillared layered structure of $LnK(C_4O_4)_2$

(36) Dan, M.; Rao, C. N. R. *Solid State Sci.* **2003**, *5*, 615−620.
(37) Köferstein, R.; Robl, C. *Z. Anorg. Allg. Chem.* **2003**, *629*, 371−373.
(38) Robl, C.; Weiss, A. *Z. Anorg. Allg. Chem.* **1987**, *546*, 161−168.

presents strong analogies with that recently reported for $Ba(C_4O_4)$.[37] Both phases crystallize with a tetragonal symmetry, and unit cell parameters differ only by 6.2%. The pillared structure feature has been observed in some other carboxylate compounds, e.g. in titanium(IV) oxalate,[39] in which the oxalate groups connect stacking layers made of TiO_6 octahedra. In the same manner, such architecture is a noticeable characteristic of some phosphonate-based materials, for example in ref 40.

Conclusion

A new series of mixed potassium and rare-earth squarates, $[Ln(H_2O)_6]K(H_2C_4O_4)(C_4O_4)_2$ (Ln = Y, La, Gd, Er), has been synthesized and structurally characterized. The compounds possess a bidimensional structure strengthened by van der Waals interactions and hydrogen bonds. The main interesting feature resides in squarate entities having different coordination fashions. In particular, the presence of a neutral squaric acid group involves the formation of attractive microcrystalline intermediate products observed during the thermal decomposition of the precursor. Here again, powder diffraction using laboratory X-rays plays a major role in the knowledge of the degradation processes leading to final oxides. Indeed, the decomposition scheme of $[Ln(H_2O)_6]K(H_2C_4O_4)(C_4O_4)_2$ has been enlightened by the power of thermodiffractometry. Furthermore, the structure elucidation, from powder data, of the decomposition product $LnK(C_4O_4)_2$ has been allowed by the application of advanced tools of powder crystallography. It might enrich the crystal chemistry of such materials and open the route to new organic spacers in inorganic chemistry.

Acknowledgment. The authors are grateful to Dr. D. Louër for helpful discussions. We are indebted to Dr. T. Roisnel (Centre de Diffractométrie X, Université de Rennes I), Mrs. G. Marsolier, and S. Lanoë for their assistance in single-crystal (T.R.) and powder (G.M. and S.L.) X-ray diffraction data collection.

Supporting Information Available: Crystallographic data for $[Y(H_2O)_6]K(H_2C_4O_4)(C_4O_4)_2$ in CIF format. This material is available free of charge via the Internet at http://pubs.acs.org.

IC0488839

(39) Boudaren, C.; Bataille, T.; Auffrédic, J.-P.; Louër, D. *Solid State Sci.* **2003**, *5*, 175−182.
(40) Clearfield, A. *Chem. Mater.* **1998**, *10*, 2801−2810 and references therein.